

The candy wrapper problem - a temporal multiscale approach for pde/pde systems

Thomas Richter ^{*} Jeremi Mizerski [†]

February 25, 2020

We describe a temporal multiscale approach for the simulation of long-term processes with short-term influences involving partial differential equations. The specific problem under consideration is a growth process in blood vessels. The *Candy Wrapper Process* describes a restenosis in a vessel that has previously been widened by inserting a stent. The development of a new stenosis takes place on a long time horizon (months) while the acting forces are mainly given by the pulsating blood flow. We describe a coupled pde model and a finite element simulation that is used as basis for our multiscale approach, which is based on averaging the long scale equation and approximating the fast scale impact by localized periodic-in-time problems. Numerical test cases in prototypical 3d configurations demonstrate the power of the approach.

1 Introduction - The candy wrapper problem

The idea of opening or dilating occluded or narrowed coronary artery originates in the works of Andreas Gruentzig. First human application of percutaneous transluminal coronary angioplasty (PTCA) had been performed on September 16th 1977 at University Hospital in Zurich. The method was basically just putting the balloon catheter through narrowing and inflating it [24]. The immediate results were good, only about 1% of the patients suffered from immediate vessel closure and myocardial infarct. Later after the interventions 30% of the stenosis recurred accompanied by the symptoms of angina of the intensity close to those from before the intervention. That happened usually from 30 days to 6 months from the intervention [9]. At that time the cardiologists were convinced that only about 10% of all the patients will be suitable for the method and the rest of coronary artery disease cases had to be referred to cardiac surgery for by-pass grafting. The remedy for the situation were to be stents intended as an internal scaffold for the artery to maintain its patency. The method was introduced in 1986 with some success [15]. Soon after that a new set of complications came into the attention. The early and late onset of thrombosis

^{*}University of Magdeburg, Universitätsplatz 2, 39104 Magdeburg, Germany, thomas.richter@ovgu.de

[†]University of Magdeburg, Universitätsplatz 2, 39104 Magdeburg, Germany, jeremi.mizerski@ovgu.de

started to haunt the patients undergoing procedures of bare metal stent (BMS) implantation. The BMS coped also with the problem of intimal hypertrophy which resulted in in-stent stenosis. From that moment on the era of drug eluting stents (DES) begins. Throughout the 90s different companies try different chemical compounds. The first successful application was reported by Serruys in 1998 [14]. That however did not solve the problem entirely and resulted in even more complex set of complications [1, 34]. The platelet dependent thrombosis resulted in explosion of anti-platelet drug development in following years. The problem defined as a “restenosis of treatment margins” or “candy wrapper” phenomenon was described by radiologists trying to apply the oncological brachytherapy principles to the neointimal overgrowth inside BMS [12]. Soon after that the molecular bases of the process started to be extensively studied [8]. The issue of stent edge stenosis had not been resolved by introduction of new materials and coatings [11, 10]. The biological effects of flow properties have been studied extensively since the introduction of extracorporeal circulatory system in early 50s. The body of evidence built on that experience showed large interdependencies between the local flow properties and the tissue response. The research areas branched towards optimization of stent struts geometry [31] and usage of different cytostatic drugs as a stent coating material [23]. The key elements of the milieu created by stents are usually considered separately. Some computational models allow to recreate and integrate more elements into the system [30, 41]. By means of computer simulations the researchers were able to simulate not only fluid dynamics around the stented area but also the effects of drug diffusion into the arterial walls [3, 44]. The edge restenosis phenomenon however did not find its conclusive description. To fully understand that complex phenomenon we need to take the arterial wall mechanics and fluid-structure interactions into consideration. The specific challenge that is tackled in this work is the temporal multiscale character of this problem: While restenosis occurs after months, the driving mechanical forces come from the pulsating blood flow that requires a resolution in the order of centiseconds. Direct simulations of this long-term process are not feasible and we present temporal multiscale methods aiming efficient predictions.

2 Model configuration

In this section we will briefly describe the mathematical model used to describe the stenosis growth effects. Medical, biological and chemical processes are strongly simplified. They do however still contain the specific couplings and scales that are characteristic for the underlying problem. We choose problem parameters as close to the medical configuration as possible and as known, which is an issue since good data is difficult to measure and only sparsely available.

The most important simplification in our present computational model is the assumption of a rigid vessel wall. Although deformation by dynamical fluid-structure interactions are small it is well known that the effects of elasticity should be taken into effect for an appropriate depiction of wall stresses, which are an essential ingredient in triggering stenosis growth. However, we give an outlook on techniques that are suitable to substantially increase the efficiency in medical fluid-structure interaction simulation that suffer from special instabilities by the added-mass effect due to similar masses of fluid and solid [7].

2.1 Governing equations

We consider a system of partial differential equations that is inspired by [42, 43], where a complex system of partial differential equations describing the interaction of mechanical fluid-structure interactions with bio/chemical reactions and active growth and material deformation is introduced. The mechanical system is described by a nonlinear fluid-structure interaction model, where the blood is modeled as incompressible Newtonian fluid, which is an adequate choice for the vessel sizes under consideration

$$\rho_f (\partial_t \mathbf{v} + (\mathbf{v} \cdot \nabla) \mathbf{v}) - \operatorname{div} \boldsymbol{\sigma}(\mathbf{v}, p) = 0, \quad \operatorname{div} \mathbf{v} = 0 \text{ in } \mathcal{F}(t), \quad (1)$$

where $\mathcal{F}(t)$ is the (moving) fluid domain, the lumen, $\rho_f \approx 1.06 \text{ gcm}^{-3}$ the density of the blood and $\boldsymbol{\sigma}(\mathbf{v}, p) = \rho_f \nu_f (\nabla \mathbf{v} + \nabla \mathbf{v}^T) - pI$ the Cauchy stress tensor, depending on velocity \mathbf{v} and pressure p , with the kinematic viscosity $\nu_f \approx 0.03 \text{ cm}^2\text{s}^{-1}$. The vessel walls are governed by an elastic material

$$J \rho_s \partial_t \mathbf{v} - \operatorname{div} (\mathbf{F} \boldsymbol{\Sigma}) = 0, \quad \mathbf{v} = \partial_t \mathbf{u} \text{ in } \mathcal{S}, \quad (2)$$

where ρ_s is the fluid's density (in current configuration), \mathbf{v} the velocity, \mathbf{u} the deformation, $\mathbf{F} := I + \nabla \mathbf{u}$ the deformation gradient with determinant $J := \det \mathbf{F}$. By \mathcal{S} we denote the Lagrangian reference configuration. By $\boldsymbol{\Sigma}$ we denote the Piola Kirchhoff stresses. The proper modeling of the stresses within vessel walls is under active research [27]. In particular there is still little knowledge on the degree of complexity that is required for accurately predicting the behavior of the coupled system. To incorporate growth of the stenosis in the context of fluid-structure interactions, the technique of a multiplicative decomposition of the deformation gradient

$$\mathbf{F} = \mathbf{F}_e \mathbf{F}_g(c), \quad \mathbf{F}_e = \mathbf{F} \mathbf{F}_g(c)^{-1}, \quad V_0 \xrightarrow{\mathbf{F}_g} V_g \xrightarrow{\mathbf{F}_e} V$$

into active deformation $\mathbf{F}_g(c)$ and elastic response \mathbf{F}_e can be applied, see [40, 20]. The idea is to introduce an intermediate configuration that includes the growth $\hat{\mathcal{S}} \rightarrow \hat{\mathcal{S}}_g$ and that is mediated by $\mathbf{F}_g(c)$ depending directly on the exterior growth trigger c but that is not physical, i.e. it is stress free but not necessarily free of strain. The stresses then depend on the elastic part only, to be precise on $\mathbf{F}_e = \mathbf{F}_g(c)^{-1}(I + \nabla \mathbf{u})$. Such models are successfully used in describing the formation of plaques [42, 43].

In this work we considerably simplify the model by neglecting all elastic effects. The Navier-Stokes equations are solved in the domain \mathcal{F} that directly depends on a growth variable c by prescribing normal growth

$$\partial \mathcal{F}(c(t)) = \{\mathbf{x} - c(\mathbf{x}, t) \cdot \vec{n}_{\hat{\mathcal{F}}}(\mathbf{x}) : \mathbf{x} \in \partial \hat{\mathcal{F}}\},$$

where $\hat{\mathcal{F}}$ is the non-grown fluid domain in reference state and $\vec{n}_{\hat{\mathcal{F}}}$ the outward facing unit normal vector. The description of the coupled problem we will be based on an ALE formulation, where all quantities are given on the undeformed reference domain $\hat{\mathcal{F}}$, see [36, Chapter 5]. This reference domain is a straight pipe of length 7 cm and diameter 0.2 cm. A typical curvature, irregularities, the effect of the stent and in particular of the stenosis will be augmented by the ALE deformation $T(t) : \hat{\mathcal{F}} \rightarrow \mathcal{F}(t)$.

The growth variable c will live on the surface $\partial\hat{\mathcal{F}}$. The evolution of c is governed by a simple surface diffusion equation

$$d_t c - \lambda_c \Delta_\Gamma c = R(c, \boldsymbol{\sigma}) \text{ on } \partial\hat{\mathcal{F}}, \quad (3)$$

with the Laplace Beltrami operator Δ_Γ and a small diffusion constant $\lambda_c \approx 5 \cdot 10^{-7} \text{ m}^2/\text{s}$. Due to the very slow evolution of the plaque, the motion of the evolving surface can be neglected in the temporal derivative. There is no experimental data on the role of diffusion and the size of λ_c . We will hence consider λ_c as a procedure for stabilization and choose is small enough to cancel any effects on the macroscopic evolution of the growth. In lack of relevant parameters equation (3) can be considered to be dimensionless. By $R(c, \boldsymbol{\sigma})$ we denote the coupling term triggering growth of the stenosis

$$R(c, \boldsymbol{\sigma}; \mathbf{x}) = \frac{\alpha}{1 + \beta c(\mathbf{x})} \gamma(\sigma_{WSS}(\boldsymbol{\sigma}(\mathbf{x}); \mathbf{x})). \quad (4)$$

The parameter α controls the rate of the stenosis growth and it can be considered as the scale parameter separating the fast scale of the fluid problem from the slow scale of the growth, by β we control some saturation of the growth. By σ_{WSS} we denote the wall shear stress that is acting close to the tips of the stent at s_0 and s_1 (in direction of the main flow direction \mathbf{x}_1 , where injuring of the vessel wall will trigger stenosis growth

$$\sigma_{WSS}(\boldsymbol{\sigma}; \mathbf{x}) = |\boldsymbol{\sigma}(\mathbf{x}) \vec{n}(\mathbf{x}) \cdot \vec{n}(\mathbf{x})| \left(\Theta(s_0; \mathbf{x}_1) + \Theta(s_1; \mathbf{x}_2) \right),$$

with

$$\Theta(s; x) = \left(1 + \exp(2(s_0 - 1 - x)) \right)^{-1} \left(1 + \exp(2(x - s_0 - 1)) \right)^{-1}.$$

Only wall shear stresses in a certain range above and below activation limits are responsible for plaque growth, hence we introduce the scaling function $\gamma(\cdot)$ as

$$\gamma(S) = \left(1 + \exp(3(\sigma_{min} - S)) \right)^{-1} \left(1 + \exp(3(S - \sigma_{max})) \right)^{-1}.$$

2.2 Parameters

All computations are carried out on the reference domain, a vessel of diameter 0.2cm and length 7cm. Deformations, imposed by the stent T_{stent} , the general curvature of the configuration $T_{geometry}$ and the stenosis $T_{stenosis}$ are realized by mappings

$$T = T_{geometry} \circ T_{stenosis} \circ T_{stent}.$$

All units are given in cm, g, s.

T_{stent} models the impact of the stent, a slight extension of the vessel at the tips s_l and s_r .

$$T_{stent}(x) = \begin{pmatrix} x_1 \\ 0 \\ 0 \end{pmatrix} + \left(1 + \rho_{stent} e^{-\gamma_{stent}(x_1 - s_0)^2} + e^{-\gamma_{stent}(x_1 - s_1)^2} \right) \begin{pmatrix} 0 \\ x_2 \\ x_3 \end{pmatrix} \quad (5)$$

with $\rho_{stent} = 0.1$ and $\gamma_{stent} = 50$. Growth of the stenosis is assumed to be in normal direction only. We prescribe $T_{stenosis}$ by the simple relation

$$T_{stenosis}(c; x) = \begin{pmatrix} x_1 \\ 0 \\ 0 \end{pmatrix} + (1 - c(x)) \begin{pmatrix} 0 \\ x_2 \\ x_3 \end{pmatrix}.$$

The overall vessel geometry is curved in the x/y plane for $x_1 < s_m = 3.5$ cm which is the left half of the vessel and in the x/z plane for $x_1 > s_m$

$$T_{geo}(x) \Big|_{x_1 < s_m} = \begin{pmatrix} x_1 - \tau(x_1)(1 + \tau(x_1)^2)^{-\frac{1}{2}} x_2 \\ \tau'(x_1) + (1 + \tau(x_1)^2)^{-\frac{1}{2}} x_2 \\ x_3 \end{pmatrix}, \quad T_{geo}(x) \Big|_{x_1 > s_m} = \begin{pmatrix} x_1 - \tau(x_1)(1 + \tau(x_1)^2)^{-\frac{1}{2}} x_3 \\ x_2 \\ \tau'(x_1) + (1 + \tau(x_1)^2)^{-\frac{1}{2}} x_3 \end{pmatrix}$$

where $\tau(x_1)$ describes the center-line of the deformed vessel, given by $\tau(x_1) = 4 \cdot 10^{-3}(x_1 - s_m)^4$. The mapping is chosen to give a curvature that is realistic in coronary arteries with a straight middle-section describing the stented area. As further parameters we consider the fluid density $\rho_f = 1.06 \text{ g} \cdot \text{cm}^{-3}$, the viscosity $\nu = 0.03 \text{ cm}^2 \cdot \text{s}^{-1}$. The stent starts at $s_0 = 2$ cm, extends over 3 cm to $s_1 = 5$ cm. The geometric parameters for the impact of the stent, see 5, are $\gamma_{stent} = 50$ and finally, the reaction term uses the limits $\sigma_{min} = 5$ and $\sigma_{max} = 8$.

The flow problem is driven by enforcing a periodic relative pressure profile (inflow to outflow) condition that is inspired from the usual pressure drops in stented coronary arteries suffering from a stenosis. On the inflow boundary Γ_{in} we prescribe the time-periodic average pressure

$$P_{in}(t) = \begin{cases} 10 + 25t & 0 \leq t < 0.4 \text{ s} \\ 140/3 - 200t/3 & 0.4 \text{ s} \leq t < 0.7 \text{ s}, \quad \text{periodically extended over } [0, 1] \\ 100/3t - 70t/3 & 0.7 \text{ s} \leq t < 1 \text{ s} \end{cases}$$

2.3 ALE Formulation and Discretization

Based on the mapping $T(x) = T_{geometry}(x) \circ T_{stenosis}(x) \circ T_{stent}(x)$ the Navier-Stokes equations and the surface growth equation are transformed to ALE coordinate, e.g. by introducing reference values $\hat{v}(\hat{x}, t) = v(x, t)$, $\hat{p}(\hat{x}, t) = p(x, t)$ and $\hat{c}(\hat{x}, t) = c(x, t)$. The resulting set of equations is given on the reference domain $\hat{\mathcal{F}}$ and in variational formulation it takes the form

$$\begin{aligned} & \left(J \rho_f (\partial_t \hat{v} + (\hat{\mathbf{F}}^{-1} \hat{v} \cdot \hat{\nabla}) \hat{v}), \phi \right)_{\hat{\mathcal{F}}} + \left(J \hat{\sigma} \mathbf{F}^{-T}, \hat{\nabla} \hat{\phi} \right)_{\hat{\mathcal{F}}} = 0 \\ & \left(J \mathbf{F}^{-1} : \hat{\nabla} \hat{v}, \xi \right)_{\hat{\mathcal{F}}} = 0, \quad \left(c', \psi \right)_{\hat{\partial \mathcal{F}}} + \left(\lambda_c \nabla_{\Gamma c}, \nabla_{\Gamma} \psi \right)_{\hat{\partial \mathcal{F}}} = R(\hat{c}, \hat{\sigma}). \end{aligned} \quad (6)$$

Several simplifications in comparison to an exact ALE formulation have been applied: due to the very slow evolution of the surface we neglect inertia terms by its motion. Further, since surface diffusion will only serve as numerical stabilization we refrain from an exact transformation of the surface Laplace.

The discretization of system (6) is by standard techniques. In time, we use the θ -time stepping method

$$u' = f(t, u) \quad \rightarrow \quad u_n - u_{n-1} = \Delta t \theta f(t_n, u_n) + \Delta t (1 - \theta) f(t_{n-1}, u_{n-1}),$$

with constant step sizes Δ and the choice $\theta = \frac{1}{2} + O(k)$ to achieve second order accuracy with good stability properties, see [32, 38]. Spatial discretization is by means of stabilized equal order tri-quadratic finite elements on a hexahedral mesh. For stabilization of the inf-sup condition and of convective regimes the local projection stabilization is used [4, 5]. The surface pde is continued into the fluid domain and can be considered as a weakly imposed boundary condition. We refer to [36] for details on the discretization and implementation in Gascoigne 3D [6].

3 Temporal multiscales

The big challenge of the candy wrapper problem is in the range of temporal scales that must be bridged. While the flow problem is driven by a periodic flow pattern with period 1 s the growth of the stenosis takes months. The growth model comprises the parameter α , see (4) that indicates exactly this scale separation, since $|R(c, \sigma)| = O(\alpha)$. In [19] we have recently introduced and analysed a temporal multiscale scheme for exactly such long-scale / short-scale problems governed by a pde/ode system and driven by a periodic-in-time micro process. Here we extend this technique for handling 3d pde/pde couplings.

We briefly sketch the layout of the multiscale approximation. To begin with, we identify the growth parameter $c(\mathbf{x}, t)$ as the main variable of interest. Furthermore, as we are interested in the long term behavior of the growth only, we introduce the (locally) averaged growth variable

$$\bar{c}(\mathbf{x}, t) = \int_t^{t+1} c(\mathbf{x}, s) ds, \quad (7)$$

where the averaging extends over one period only.

Next, to decouple slow and fast scales we make the essential assumption that the flow problem on a fixed domain $\mathcal{F}(\bar{c}_f)$, where $\bar{c}_f := \bar{c}(t_f)$ for one point in time t_f admits a periodic in time solution

$$\begin{aligned} & \left(J(\bar{c}_f) \rho_f (\partial_t^{\bar{c}_f} \mathbf{v}^{\bar{c}_f} + (\mathbf{F}(\bar{c}_f)^{-1} \mathbf{v}^{\bar{c}_f} \cdot \nabla) \mathbf{v}^{\bar{c}_f}), \phi \right)_{\mathcal{F}} \\ & + \left(J(\bar{c}_f) \sigma^{\bar{c}_f} \mathbf{F}(\bar{c}_f)^{-T}, \nabla \phi \right)_{\mathcal{F}} + \left(J(\bar{c}_f) \mathbf{F}(\bar{c}_f)^{-1} : \nabla \mathbf{v}^{\bar{c}_f}, \xi \right)_{\mathcal{F}} = 0 \\ & \mathbf{v}^{\bar{c}_f}(\cdot, 0) = \mathbf{v}^{\bar{c}_f}(\cdot, 1) \end{aligned} \quad (8)$$

Only very few theoretical results exist on periodic solutions to the Navier-Stokes equations, see [21]. They only hold in the case of small data which is not given in the typical candy wrapper configurations with Reynolds numbers going up to about $Re = 1000$. Computational experiments however do suggest the existence of stable periodic solutions in the regime of interest.

Multiscale Algorithm Given such periodic solutions, the computational multiscale method is based on a subdivision of $I = [0, T]$ (where $T \approx$ months is large) into macro time-steps t_n for $n = 0, \dots, N$ with $t_0 = 0$ and $T_N = T$ and the step size $K = t_n - t_{n-1}$. The small interval of periodicity $I_P = [0, 1]$ is partitioned into micro time-steps τ_n for $n = 0, \dots, M$ with $\tau_0 = 0$, $\tau_M = 1$ and the step size $k = \tau_m - \tau_{m-1} \ll K$. A simple explicit/implicit multiscale iteration is then as follows:

Algorithm 1 (First order explicit/implicit multiscale iteration) Let \bar{c}_0 be the initial value for the slow component. For $n = 1, 2, \dots$ iterate

1. Solve the periodic flow problem $(\mathbf{v}^{\bar{c}_{n-1}}, p^{\bar{c}_n})$ on the domain $\mathcal{F}(\bar{c}_{n-1})$
2. Compute the average of the reaction term

$$\begin{aligned}\bar{R}(\bar{c}_{n-1}) &:= \int_0^1 R(\bar{c}_{n-1}, \boldsymbol{\sigma}^{\bar{c}_{n-1}}(s); \mathbf{x}) ds \\ &= \frac{\alpha}{1 + \beta \bar{c}_{n-1}(\mathbf{x})} \int_0^1 \gamma(\boldsymbol{\sigma}_{WSS}(\boldsymbol{\sigma}^{\bar{c}_{n-1}}(\mathbf{x}, s); \mathbf{x})) ds\end{aligned}$$

3. Make an semi-explicit step of the stenosis growth problem

$$K^{-1}(\bar{c}_n - c_{n-1}, \psi)_{\partial \hat{\mathcal{F}}} + (\lambda_c \nabla_{\Gamma} \bar{c}_n, \nabla_{\Gamma} \psi)_{\partial \hat{\mathcal{F}}} = (\bar{R}(\bar{c}_{n-1}), \psi)_{\partial \hat{\mathcal{F}}}$$

The discretization of the growth problem in Step 3. can easily be replaced by a second order explicit scheme like the Adams-Bashforth formula, see [19]. A fully implicit time-integration can be realized by adding a sub-iteration for steps 2-4. However, since the diffusion parameter is very small, explicit schemes are appropriate in this setting.

Within every step of the iteration it is necessary to solve the periodic-in-time flow problem (even multiple solutions are required in a fully implicit setting). This is the main effort of the resulting scheme, since the sub interval $[0, 1]$ must be integrated several times to obtain a suitable periodic solution. In principle it is possible to just compute several cycles of the periodic problem until the periodicity error

$$\|\mathbf{v}^{\bar{c}_n}(T + 1 \text{ s}) - \mathbf{v}^{\bar{c}_n}(T)\| < \epsilon_P$$

falls below a given threshold $\epsilon_P > 0$. Usually however this error is decreasing with an exponential rate only that depends on parameters like the viscosity and the domain size. For acceleration several methods are discussed in literature, based on optimization problem [39], on the idea of the shooting method [28], on Newton [25] or on space time techniques [33]. Here we quickly present a very efficient novel scheme that converges with a fixed rate that does not depend on any further parameters. We note however that although the computational efficiency is striking, the theoretical validation extends to the linear Stokes equation only, see [37].

Solution of the periodic flow problem The idea of the averaging scheme for the rapid identification of periodic flow problems is to split the periodic solution into average and oscillation, see also [37]

$$\mathbf{v}^{\pi}(t) = \bar{\mathbf{v}}^{\pi} + \tilde{\mathbf{v}}^{\pi}(t), \quad \int_0^1 \tilde{\mathbf{v}}^{\pi}(s) ds = 0.$$

In a nonlinear problem like the Navier-Stokes equations it is not possible to separate the average from the oscillations. But, by averaging the Navier-Stokes equation, we derive

$$-\operatorname{div} \bar{\boldsymbol{\sigma}}_f^{\pi} + (\bar{\mathbf{v}}^{\pi} \cdot \nabla) \bar{\mathbf{v}}^{\pi} = - \underbrace{\int_0^1 \left\{ (\tilde{\mathbf{v}}^{\pi}(s) \cdot \nabla) \bar{\mathbf{v}}^{\pi} + (\bar{\mathbf{v}}^{\pi} \cdot \nabla) \tilde{\mathbf{v}}^{\pi}(s) \right\} ds}_{=: N(\bar{\mathbf{v}}^{\pi}, \tilde{\mathbf{v}}^{\pi})}, \quad \operatorname{div} \bar{\mathbf{v}}^{\pi} = 0.$$

If we average a solution $(\mathbf{v}(t), p(t))$ to the Navier-Stokes problem for arbitrary initial \mathbf{v}_0 (that does not yield the periodic solution) we get

$$-\operatorname{div} \bar{\sigma}_f + (\bar{\mathbf{v}} \cdot \nabla) \bar{\mathbf{v}} = \mathbf{v}(0) - \mathbf{v}(1) + N(\bar{\mathbf{v}}, \bar{\mathbf{v}}), \quad \operatorname{div} \bar{\mathbf{v}} = 0.$$

The difference $\mathbf{w} := \mathbf{v}^\pi - \mathbf{v}$, $q := p^\pi - p$ between dynamic solution and periodic solution satisfies the averaged equation

$$\begin{aligned} -\operatorname{div} \bar{\sigma}_f(\bar{\mathbf{w}}, \bar{q}) + (\bar{\mathbf{w}} \cdot \nabla) \bar{\mathbf{w}} + (\mathbf{w} \cdot \nabla) \bar{\mathbf{v}} + (\bar{\mathbf{v}} \cdot \nabla) \mathbf{w} \\ = \mathbf{v}(1) - \mathbf{v}(0) + N(\bar{\mathbf{v}}^\pi, \bar{\mathbf{v}}^\pi) - N(\bar{\mathbf{v}}, \bar{\mathbf{v}}), \quad \operatorname{div} \bar{\mathbf{w}} = 0. \end{aligned}$$

We assume that we start with a good guess \mathbf{v} that is already close to the periodic solution \mathbf{v}^π , i.e. $\|\mathbf{w}\|$ is small. If no initial is available, e.g. in the very first step of the multiscale scheme, we still can perform a couple for forward simulations. Given that $\|\mathbf{w}\|$ is small, we will neglect both the nonlinearity $(\bar{\mathbf{w}} \cdot \nabla) \bar{\mathbf{w}}$ and all fluctuation terms $N(\cdot, \cdot)$ involving the oscillatory parts. We approximate the difference between average of the dynamic solution and average of the desired periodic solution by the linear equation

$$(\mathbf{w} \cdot \nabla) \bar{\mathbf{v}} + (\bar{\mathbf{v}} \cdot \nabla) \mathbf{w} - \operatorname{div} \bar{\sigma}_f(\bar{\mathbf{w}}, \bar{q}) = \mathbf{v}(1) - \mathbf{v}(0) \quad (9)$$

The averaging scheme for finding the periodic solution is then given by the following iteration.

Algorithm 2 (Averaging scheme for periodic-in-time problems) *Let \mathbf{v}_0^0 be a guess for the initial value. If no approximation is available, \mathbf{v}_0^0 can be obtained by computing several cycles of the dynamic flow problem. For $l = 1, 2, \dots$ iterate*

1. *Based on the initial $\mathbf{v}^l(0) = \mathbf{v}_0^{l-1}$ solve once cycle of the dynamic flow problem on $I_P = [0, 1]$.*
2. *Solve the averaging equation for $\bar{\mathbf{w}}^l$ and \bar{q}^l , equation (9)*
3. *Update the initial value by correcting the average*

$$\mathbf{v}_0^l := \mathbf{v}^l(1) + \bar{\mathbf{w}}^l.$$

The analysis of this averaging scheme is open for the Navier-Stokes equations but simple for linear problems with symmetric positive definite operator like the Stokes equations. Here the convergence estimate

$$\|\mathbf{v}_0^l - \mathbf{v}_0^\pi\| \leq \rho_{avg} \cdot \|\mathbf{v}_0^{l-1} - \mathbf{v}_0^\pi\|$$

holds, with $\rho_{avg} < 0.3$ in the continuous and $\rho_{avg} < 0.42$ in the discrete setting, for further results we refer to [37].

4 Numerical results

We present a numerical study on the multiscale scheme and give a first discussion on its accuracy and efficiency. In [19] simpler two dimensional problems have been studied that also allow for

ν	0.1	0.05	0.025		0.1	0.05	0.025
	forward				averaging		
cycles	40	74	140		15	15	18

Table 1: Number of cycles required to reduce the periodicity error to $\|\mathbf{v}(t + 1 \text{ s}) - \mathbf{v}(t)\| < 10^{-8}$ for the direct forward simulation and the averaging scheme. Variation in the viscosity ν .

resolved simulations such that a direct comparison of computational times for forward simulations and multiscale simulations can be performed. These demonstrated speedups reaching from 1 : 200 to 1 : 10 000. Here it was shown that the multiscale scheme benefits from larger scale separation. To be precise: to reach the same relative accuracy in a multiscale computation as compared to a direct forward computation, the speedup behaves like 1 : α^{-1} .

Before presenting results for the multiscale method we briefly discuss the averaging scheme for finding periodic solutions

4.1 Convergence of the averaging scheme for periodic flow problems

We consider a 3d problem that is inspired by the driven cavity problem. On the cube $\Omega = (-2, 2)^3$ we drive the Navier-Stokes equation by a 1-periodic forcing

$$\mathbf{f}(\mathbf{x}, t) = \frac{\sin(2\pi t)}{6} \begin{pmatrix} 3 \tanh(\mathbf{x}_2) \\ 2 \tanh(\mathbf{x}_3) \\ \tanh(\mathbf{x}_1) \end{pmatrix}$$

Since the data is periodic in time we can expect to obtain a time-periodic solution (if the Reynolds number is sufficiently small). In Tab. 1 we show the performance of the averaging scheme in comparison to a simple forward iteration. We give the number of cycles required to reach the periodicity error $\|\mathbf{v}(T_n + 1 \text{ s}) - \mathbf{v}(T_n)\| < 10^{-8}$. The results show a strong superiority of the averaging scheme, both in terms of robustness (with respect to ν) and in terms of the overall computational complexity. For the forward iteration, the number of cycles approximately doubles with each reduction of ν . The performance of the averaging scheme slightly deteriorates for $\nu = 0.025$ due to the higher Reynolds number regime. For $\nu = 0.01$ we cannot identify a stable periodic solution. The computational overhead of the averaging scheme is very low, one additional stationary problem must be solved in each cycle. A detailed study of the averaging scheme with an analysis of the sensitivity to various further parameters is given in [37].

4.2 Simulation of the candy wrapper problem

Fig. 1 shows the evolution of the stenosis at three different points in time. In addition we show the outflow rate as function over time (one period). Several effects known from the medical practice can be identified: The growth of the stenosis is non-symmetric and mostly centered on the inflow-tip of the stent. This shows the necessity of considering full three dimensional models. Further, the simulations show an extension and growth of the stenosis to both sides which is also

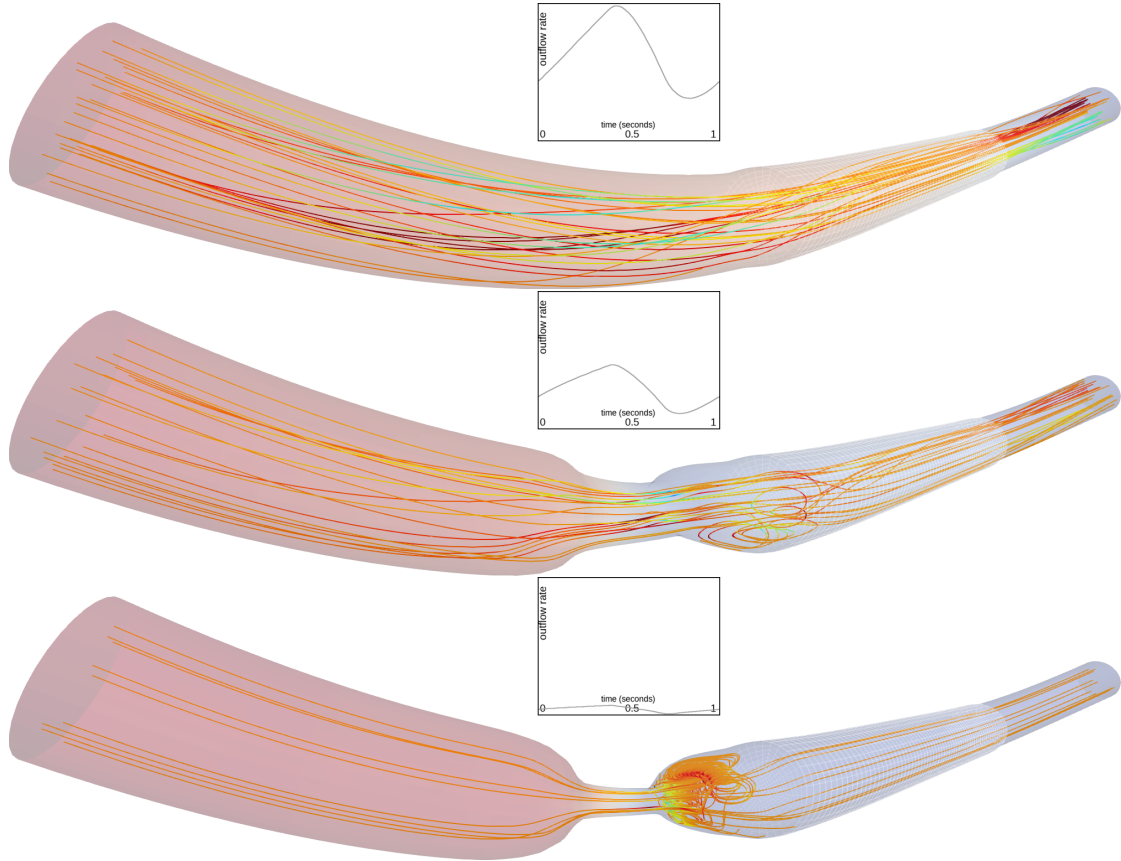


Figure 1: Development of the stenosis at initial time, at $T = 33$ days and $T = 67$ days. The average and the oscillation of the flow rate get smaller while the stenosis develops.

typical. Since the flow is pressure driven, the outflow rate decreases with the development of the stent.

In Table 2 we compare the results of the multiscale scheme for different values of k and K . We observe convergence in both parameters. Numerical extrapolation yields $\mathcal{O}(k^{1.58} + K^{1.58})$, slightly off the expected rates $\mathcal{O}(k^2 + K)$. We also indicate the computational times required for running the multiscale scheme till $T \approx 18$ days. A corresponding resolved simulation would require about 55 years computational time. This value is predicted based on the average time for computing a complete cycle of the periodic problem and based on an average three iterations required for approximating the periodic flow problem. Assuming that the extrapolated value for $K \rightarrow 0$ is accurate, the simulation based on $K \approx 36\,000$ s carries a multiscale error of about 1%. This approximation is achieved in 40 min instead of 55 years. The results in Table 2 indicate that it is worthwhile to consider a second order time stepping scheme for the plaque growth problem, since the error in K dominates. We refer to [19] for a realization in the context of a pde / ode long-scale / short scale problem.

K	k	J_{out}	time	K	k	J_{out}	time
144 000	0.02	0.9359	9 min	72 000	0.04	0.9132	15 min
72 000	0.02	0.9138	18 min	72 000	0.02	0.9138	18 min
36 000	0.02	0.9043	40 min	72 000	0.01	0.9140	41 min
extra $K \rightarrow 0$		0.8971 (1.22)	55 years ^(*)	extra $k \rightarrow 0$		0.9131 (1.58)	

Table 2: Outflow J_{out} at time $T \approx 18$ days and extrapolation including numerical convergence order for $K \rightarrow 0$ (k fixed) and $k \rightarrow 0$ (K fixed). 55 years (*) computational time result from a projection of the computational time for a resolved simulation without the multiscale scheme.

5 Outlook and discussion

We have demonstrated a numerical framework for simulating complex multiphysics / multiscale problems in hemodynamics. For the first time we could demonstrate an efficient numerical scheme for a long-scale / short-scale problem coupling different partial differential equations. We are able to include both temporal and spatial effects in bio-medical growth applications. The combination of a temporal multiscale method with fast solvers and efficient discretizations for the (periodic) micro problems gives substantial speedups such that three dimensional problems can be treated. Two main challenges remain for future work:

Fluid-structure interactions The main challenge in including elastic vessel walls lies in the increased complexity of the resulting system due to nonlinearities coming from the domain motion and the coupling to the hyperbolic solid equation that, by introducing the deformation as additional variable, blows up the problem size. In hemodynamical applications the coupling is governed by the added mass instability that usually calls for strongly coupled solution approaches, see [7, 26]. Although some progress has been made in recent years [35, 2, 29, 18], the design of efficient solvers for the resulting algebraic problems is still not satisfactory.

Considering monolithic solution approaches in combination with Newton-Krylov solvers make the use of large time steps possible. In all of the just mentioned approaches for designing linear solvers it has shown to be essential to partition the linear system when it actually comes to inversion of matrices, either within a preconditioner or within a multigrid smoother. This is mainly due to the very large condition numbers of the coupled system matrix that by far exceeds those of the subproblems, see [35, 2].

A second difficulty coming with fluid-structure interactions lies in the derivation of the effective growth equation described in Section 3. If elastic fluid-structure interactions are taken into account, the domain undergoes oscillations in the scale of the fast problem, i.e. during each pulsation of the blood flow. However, we can nevertheless introduce the averaged growth variable $\bar{c}(\mathbf{x}, t)$ as in (7) and simply average the growth equation, the this equation of Eq. (6) as this is stated on the fixed reference domain. We note however that we have chosen a very simple growth model given as surface equation. Considering the detailed system introduced in [42], growth takes place within the solid, which is a three dimensional domain $S(t) \subset \mathbb{R}^3$ undergoing deformation from

the coupled fsi problem. A corresponding equation mapped to the fixed reference domain $\hat{\mathcal{S}}$ (taken from [42]) reads

$$\left(\frac{\partial}{\partial t}(J\hat{c}), \psi \right)_{\hat{\mathcal{S}}} + \left(\lambda_c J \mathbf{F}^{-1} \mathbf{F}^{-T} \nabla \hat{c}, \nabla \psi \right)_{\hat{\mathcal{S}}} = R(\hat{c}, \hat{\sigma}).$$

Since J and \mathbf{F} oscillate with the frequency of the fast scale problem, derivation of an effective equation is still subject to future work.

Patient specific simulation The second open problem is to incorporate patient specific data into the simulations for generating specific predictions. Flow and geometry data can easily be measured during the stenting process. This process however is strongly invasive and causes subsequent adaptations of the vessel and the surrounding tissue interacting with the stent. Further data on the resulting configurations are not easily available without additional interventions. With a diameter of only a few millimeters, coronary arteries are small, such that measurements at good accuracy cannot be obtained.

Medical application The edge stenosis accompanying the implementation of DES (Drug Eluting Stents) is great starting point for development of the further numerical experiments in the field of the plaque formation and biochemical processes ongoing in the vessel walls exposed to other types of interventions. Explosive growth of the intravascular interventions in recent decade is, inevitably, going to demand more advanced studies on the nature of vascular wall response to the implantable devices [13]. Novel numerical methods may also shade new light on well-established surgical procedures and augment the awareness of the potential benefits or hazards that are not yet fully understood or identified [16]. On the other hand the population of the patients is changing dramatically and that process is soon to accelerate. According to the recent report published by European Commission, diseases of the circulatory system are the most common cause of death in elderly population aged over 75 years [17]. In addition to that gruesome information the ageing of the European population in the years to come is growing concern of the governments. Poland belongs to the group of the countries that may become affected by the population ageing the most [22]. Due to that we face the necessity of development the most efficient treatment strategies for the elderly population. One of those treatment procedures is TAVR (Transcatheter Aortic Valve Replacement). The procedure addresses aortic valve stenosis that is quite often ailment in the aforementioned group of patients. By application of the fluid structure interaction methods it might be possible to tailor the design of the medical devices to the stiffer tissues usually present in the elderly patients in the way that may augment long time outcome of the procedure. Just such a small improvement may diminish the risk of repeated procedures undertaken in frail patients.

The methodology presented in our work should also find its application in optimization of the classic surgery for the coronary artery disease. The position of the vascular anastomosis in relation to the existing vascular wall lesions may find new rationale when understood through the knowledge of the mechanotransduction phenomena. Also the strategic planning of the target vessels and “landing sites” for the aorto-coronary by-pass grafts may find its’ new understanding. Those perspective studies could be undertaken only by the means of model based planning.

Acknowledgement

We acknowledge support by the Federal Ministry of Education and Research of Germany (project number 05M16NMA).

References

- [1] D. J. Angiolillo, M. Sabata, F. Alfonso, and C. Macaya. “candy wrapper” effect after drug-eluting stent implantation: deja vu or stumbling over the same stone again? *Catheter Cardiovasc Interv*, 61(3):387–91, 2004.
- [2] E. Aulisa, S. Bna, and G. Bornia. A monolithic ale newton-krylov solver with multigrid-richardson-schwarz preconditioning for incompressible fluid-structure interaction. *Computers & Fluids*, 174:213–228, 2018.
- [3] Brinda Balakrishnan, Abraham R. Tzafiri, Philip Seifert, Adam Groothuis, Campbell Rogers, and Elazer R. Edelman. Strut position, blood flow, and drug deposition. *Circulation*, 111(22):2958–2965, 2005.
- [4] R. Becker and M. Braack. A finite element pressure gradient stabilization for the Stokes equations based on local projections. *Calcolo*, 38(4):173–199, 2001.
- [5] R. Becker and M. Braack. A two-level stabilization scheme for the Navier-Stokes equations. In et. al. M. Feistauer, editor, *Numerical Mathematics and Advanced Applications, ENUMATH 2003*, pages 123–130. Springer, 2004.
- [6] R. Becker, M. Braack, D. Meidner, T. Richter, and B. Vexler. The finite element toolkit GASCOIGNE. [HTTP://WWW.GASCOIGNE.UNI-HD.DE](http://www.gascoigne.uni-hd.de).
- [7] P. Causin, J.F. Gerau, and F. Nobile. Added-mass effect in the design of partitioned algorithms for fluid-structure problems. *Comput. Methods Appl. Mech. Engrg.*, 194:4506–4527, 2005.
- [8] M.A. Costa and D. Simon I. Molecular basis of restenosis and drug-eluting stents. *Circulation*, 111(17):2257–2273, 2005.
- [9] D.R. Holmes et al. Restenosis after percutaneous transluminal coronary angioplasty (ptca): A report from the ptca registry of the national heart, lung, and blood institute. *The American Journal of Cardiology*, 53(12):C77–C81, 1984.
- [10] F. LaDisa J., Jr et al. Stent design properties and deployment ratio influence indexes of wall shear stress: a three-dimensional computational fluid dynamics investigation within a normal artery. *Journal of Applied Physiology*, 97(1):424–430, 2004.
- [11] L. Jian et al. An integrated taxus iv, v, and vi intravascular ultrasound analysis of the predictors of edge restenosis after bare metal or paclitaxel-eluting stents. *The American Journal of Cardiology*, 103(4):501–506, 2009.

- [12] M. Sabaté et al. Geographic miss. *Circulation*, 101(21):2467–2471, 2000.
- [13] M.J. Mack et al. Transcatheter aortic-valve replacement with a balloon-expandable valve in low-risk patients. *N. Engl. J. Med.*, 380(18):1695–1705, 2019.
- [14] P.W. Serruys et al. Randomised comparison of implantation of heparin-coated stents with balloon angioplasty in selected patients with coronary artery disease (benestent ii). *The Lancet*, 352(9129):673–681, 1998.
- [15] U. Sigwart et al. Intravascular stents to prevent occlusion and re-stenosis after transluminal angioplasty. *New England Journal of Medicine*, 316(12):701–706, 1987.
- [16] V.H. Thourani et al. Contemporary real-world outcomes of surgical aortic valve replacement in low-risk, intermediate-risk, and high-risk patients. *Ann. Thorac. Surg.*, 99(1):55–61, 2015.
- [17] EUROSTAT. Ageing europe : looking at the lives of older people in the eu. Technical report, European Union, 2019.
- [18] L. Failer and T. Richter. A parallel newton multigrid framework for monolithic fluid-structure interactions. *Journal of Scientific Computing*, accepted, 2019.
- [19] S. Frei and T. Richter. Efficient approximation of flow problems with multiple scales in time. *submitted*, 2019.
- [20] S. Frei, T. Richter, and T. Wick. Long-term simulation of large deformation, mechano-chemical fluid-structure interactions in ALE and fully Eulerian coordinates. *J. Comp. Phys.*, 321:874 – 891, 2016.
- [21] G.P. Galdi and M. Kyed. Time-periodic solutions to the navier-stokes equations. In *Giga Y., Novotny A. (eds) Handbook of Mathematical Analysis in Mechanics of Viscous Fluids*, pages 1–70. Springer, 2016.
- [22] K. Giannakouris. Ageing characterises the demographic perspectives of the european societies. In *EUROPOP2008*. European Union, 2008.
- [23] E. Grube, U. Gerckens, R. MÃijller, and L. BÃijllesfeld. Drug eluting stents: initial experiences. *Zeitschrift fÃijr Kardiologie*, 91(3):44–48, 2002.
- [24] Andreas GrÃijntzig. Transluminal dilatation of coronary-artery stenosis. *The Lancet*, 311(8058):263, 1978.
- [25] F.M. Hante, M.S. Mommer, and A. Potschka. Newton-picard preconditioners for time-periodic, parabolic optimal control problems. *SIAM J. Num. Ana.*, 53(5):2206–2225, 2015.
- [26] M. Heil, A.L. Hazel, and J. Boyle. Solvers for large-displacement fluid-structure interaction problems: Segregated vs. monolithic approaches. *Computational Mechanics*, 43:91–101, 2008.

- [27] G.A. Holzapfel. *Nonlinear Solid Mechanics: A Continuum Approach for Engineering*. Wiley-Blackwell, 2000.
- [28] L. Jiang, L. T. Biegler, and V. G. Fox. Simulation and optimization of pressure-swing adsorption systems for air separation. *AIChE Journal*, 49(5):1140–1157, 2003.
- [29] D. Jodlbauer, U. Langer, and T. Wick. Parallel block-preconditioned monolithic solvers for fluid-structure interaction problems. *International Journal for Numerical Methods in Engineering*, 117(6):623–643, 2019.
- [30] K. C. Koskinas, Y. S. Chatzizisis, A. P. Antoniadis, and G. D. Giannoglou. Role of endothelial shear stress in stent restenosis and thrombosis: pathophysiologic mechanisms and implications for clinical translation. *J Am Coll Cardiol*, 59(15):1337–49, 2012.
- [31] J.F. LaDisa, I. Guler, L.E. Olson, D.A. Hettrick, Judy R. Kersten, D.C. Warltier, and P.S. Pagel. Three-dimensional computational fluid dynamics modeling of alterations in coronary wall shear stress produced by stent implantation. *Annals of Biomedical Engineering*, 31(8):972–980, 2003.
- [32] M. Luskin and R. Rannacher. On the smoothing property of the Crank-Nicholson scheme. *Applicable Anal.*, 14:117–135, 1982.
- [33] F. Platte, D. Kuzmin, C. Fredebeul, and S. Turek. Novel simulation approaches for cyclic-steady-state fixed-bed processes exhibiting sharp fronts and shocks. In M. de Bruin, D. Mache, and J. Szabados, editors, *Trends and applications in constructive approximations*, volume 151 of *International series of numerical mathematics*, pages 207–233. Birkhäuser, 2005.
- [34] T. C. Poerner, K. K. Haase, B. Wiesinger, J. Wiskirchen, and S. H. Duda. Drug-coated stents. *Minimally Invasive Therapy & Allied Technologies*, 11(4):185–192, 2002.
- [35] T. Richter. A monolithic geometric multigrid solver for fluid-structure interactions in ALE formulation. *Int. J. Numer. Meth. Engrg.*, 104(5):372–390, 2015.
- [36] T. Richter. *Fluid-structure Interactions. Models, Analysis and Finite Elements*, volume 118 of *Lecture notes in computational science and engineering*. Springer, 2017.
- [37] T. Richter. An averaging scheme for the approximation of periodic-in-time flow problems. *submitted*, 2019.
- [38] T. Richter and T. Wick. On time discretizations of fluid-structure interactions. In T. Carraro, M. Geiger, S. Körkel, and R. Rannacher, editors, *Multiple Shooting and Time Domain Decomposition Methods*, volume 9 of *Contributions in Mathematical and Computational Science*, pages 377–400. Springer, 2015.
- [39] T. Richter and W. Wollner. Optimization framework for the computation of time-periodic solutions of partial differential equations. *Viet. J. Math.*, 46(4):949–966, 2019.

- [40] E.K. Rodriguez, A. Hoger, and A.D. McCulloch. Stress-dependent finite growth in soft elastic tissues. *J. Biomechanics*, 4:455–467, 1994.
- [41] Tuoi T. N. Vo, Sarah Morgan, Christopher McCormick, Sean McGinty, Sean McKee, and Martin Meere. Modelling drug release from polymer-free coronary stents with microporous surfaces. *International Journal of Pharmaceutics*, 544(2):392–401, 2018.
- [42] Y. Yang, W. Jäger, M. Neuss-Radu, and T. Richter. Mathematical modeling and simulation of the evolution of plaques in blood vessels. *J. of Math. Biology*, 72(4):973–996, 2016.
- [43] Y. Yang, T. Richter, W. Jaeger, and M. Neuss-Radu. An ALE approach to mechano-chemical processes in fluid-structure interactions. *Int. J. Numer. Math. Fluids.*, 84(4):199–220, 2017.
- [44] P. Zunino, C. D’Angelo, L. Petrini, C. Vergara, C. Capelli, and F. Migliavacca. Numerical simulation of drug eluting coronary stents: Mechanics, fluid dynamics and drug release. *Computer Methods in Applied Mechanics and Engineering*, 198(45):3633–3644, 2009.